

Bi-Level Coordinated Power System Restoration Model Considering the Support of Multiple Flexible Resources

Shengyuan Liu¹, Graduate Student Member, IEEE, Changming Chen¹, Yicheng Jiang, Zhenzhi Lin², Member, IEEE, Hongtao Wang¹, Senior Member, IEEE, Muhammad Waseem³, and Fushuan Wen¹, Fellow, IEEE

Abstract—When power systems encounter outages and large-scale blackouts, system restoration is critical and should be carried out with dedicated schemes. In this past, most studies divided the power system restoration into three stages (i.e., black-start zone partitioning, network reconfiguration, and load restoration) and deal with them separately. After that, few studies considering the three stages together were emerging while the support of multiple flexible resources, i.e., renewable energy source (RES), electric vehicle system (EVS) and energy storage system (ESS), were not considered comprehensively. Therefore, a bi-level coordinated power system restoration (BiCPSR) model is proposed in this work considering the support of multiple flexible resources. In the upper level, two network topology indices that describe the “reachability” and “shortest reachable distance” of buses in power systems, and the restoration characteristics of generators and loads are utilized for optimizing the start-up sequence of generators and network reconfiguration. In the lower level, the uncertainties of RES and EVS are considered by various scenarios and the support of multiple flexible resources is utilized cooperatively for accelerating the restoration process and maximizing the restorable load. Case studies on the revised IEEE 39-bus, WECC 179-bus and the actual Zhejiang power systems are performed to illustrate the basic features of the proposed model and its availability in bulk power systems. The comparisons between the proposed model and other models are also performed to illustrate the strengths of the proposed model.

Index Terms—Power system restoration, flexible resources, renewable energy source (RES), electric vehicle system (EVS) energy storage system (ESS), network topology, bi-level optimization.

I. INTRODUCTION

WITH the rapid development of control technologies and widespread application of various automatic devices in power systems, the ability of power systems to resist disturbances and failures was significantly enhanced [1]. However, due to the large-scale accommodation of intermittent and fluctuating renewable energies such as wind power and photovoltaic power into power systems, the power systems are confronted with much more complications and uncertainties, which challenge the operational securities of power systems [2]. As a result, the power systems are still at risk of entire blackouts or outages if controlled islanding fails [3], [4]. For example, a major power outage hit India in 2012, impacting more than 600 million people. In 2015, Ukraine suffered a major power outage, and more than half of its territory is affected. In 2016, a blackout occurred in South Australia and lasted more than 50 hours and millions of people were affected. In 2019, blackouts were reported in 21 states of Venezuela, which leads billions of economic losses. In February 2021, Texas announced an emergency declaration and more than 2.7 million residents lost the power supply amid an unusual cold spell, which also boosted the electricity price up to \$9000/MWh. It can be seen that a blackout or a major power outage can result in serious consequences. Therefore, it is of great theoretical and practical significance to systematically investigate the power system restoration strategies considering multiple flexible resources after partial or complete blackouts, which could guarantee the security and rapid restoration of power supply and reduce the unserved loads and financial losses.

The power system restoration can be divided into three stages (i.e., black-start zone partitioning, network reconfiguration and load restoration), and several studies have been performed on this topic. In [5], two characteristic parameters (i.e., degree and betweenness) of the complex network are used for describing the power system topologies and the community structure with modularity index is utilized for dividing interconnection into black-start zones with similar scales, which is good for the following parallel restoration. In [6], sectionalizing strategies

Manuscript received 25 November 2021; revised 21 March 2022; accepted 16 April 2022. Date of publication 28 April 2022; date of current version 27 February 2023. This work was supported by the National Natural Science Foundation of China under Grants 51777185 and 52077195. Paper no. TPWRS-01796-2021. (Corresponding author: Zhenzhi Lin.)

Shengyuan Liu is with the College of Electrical Engineering, Zhejiang University, Hangzhou 310027, China, and also with the State Grid Zhejiang Electric Power Corporation, Hangzhou 310007, China (e-mail: eelsy@zju.edu.cn).

Changming Chen, Muhammad Waseem, and Fushuan Wen are with the College of Electrical Engineering, Zhejiang University, Hangzhou 310027, China (e-mail: changmingchen@zju.edu.cn; mwaseem@zju.edu.cn; fushuan.wen@gmail.com).

Yicheng Jiang is with the State Grid Zhejiang Electric Power Corporation, Hangzhou 310007, China (e-mail: marissajyc@gmail.com).

Zhenzhi Lin is with the College of Electrical Engineering, Zhejiang University, Hangzhou 310027, China, and also with the School of Electrical Engineering, Shandong University, Jinan 250061, China (e-mail: linzhenzhi@zju.edu.cn).

Hongtao Wang is with the School of Electrical Engineering, Shandong University, Jinan 250061, China (e-mail: whtwhm@sdu.edu.cn).

Color versions of one or more figures in this article are available at <https://doi.org/10.1109/TPWRS.2022.3171201>.

Digital Object Identifier 10.1109/TPWRS.2022.3171201

based on the ordered binary decision diagram (OBDD) is proposed for parallel power system restoration, which can search several possible splitting boundaries quickly. In [7], a two-step system partitioning algorithm is proposed for parallel power system restoration. A non-black-start generator grouping model is presented in the first step to minimize its restoration time and a network sectionalizing model is presented in the second step to maximize the electrical distances and minimize the number of transmission lines among different zones. In [8], the start-up characteristics of non-black generators are considered and the start-up sequence is modeled as a mixed-integer linear programming (MILP) problem, which greatly reduces the computation burden of the enumeration method and dynamic programming. In [9], a network partitioning scheme based on propagation on the connectivity of grid, and the problem is converted into a MILP to ensure the high computational performance. In [10], a multi-time step service restoration model aiming to minimize the unserved customers is proposed for the distribution system, which is also formed as MILP and suitable for different operation conditions.

However, as mentioned in [2], most of the studies before 2015 do not consider the cooperation among black-start zone partitioning, network reconfiguration and load restoration due to the complexity. Although they can obtain relatively reasonable partitioning strategies, the ultimate goal that maximizing load restoration may not be achieved optimally.

In light of this situation, some integrated models for power system restoration are also studied [11]–[14]. In [11], a bi-level optimization model is proposed for solving the black-start zone sectionalizing problem and restoration problem, respectively. In [12], a mixed-integer programming (MIP) model is established with some criteria (e.g., self-healing time, load pickup capability, voltage stability and network observability) considered. In [13], a detailed mathematical model with generator start-up sequence, transmission network restoration and load pickup considered together is first proposed for power systems. In [14], a global optimization model considering both black-start zone partitioning and generator restarting sequence is presented and generalized Benders decomposition (GBD) is utilized to decompose the model into a master problem and two sub-problems, which can be solved iteratively. However, the aforementioned literatures do not consider the effectiveness of renewable energy sources (RES). To utilize the effectiveness of RES and deal with their uncertainty, in [15], the influence of RES is considered in the power system restoration model and the firefly algorithm (FA) is utilized for solving the nonlinear optimization problem. In [16], the influence of wind farms including their capacities, locations and control measures are discussed comprehensively, and the Latin hypercube sampling (LHS) and L-shape decomposition are utilized for characterizing the uncertainties of wind farm outputs and mitigating corresponding computation burden. In [17], [18], the characteristics of electric vehicle system (EVS) and energy storage system (ESS) are further considered, and the particle swarm optimization (PSO) method is used to handle the bi-level chance-constrained programming in [18]. In [19], the availability of power system equipment is assessed during the decision-making of power system restoration according to the

results of fault diagnosis and weather conditions, so as to determine a more practical restoration scheme in actual situations. In [20], a two-level simulation-assisted optimal sequential load restoration model for distribution system is proposed considering the dynamic frequency constraints as well as the black-start/non-black-start generators. Besides, the potential application of involving microgrids [21], [22] and distribution network [23], [24] into power system restoration in transmission level are also studied in recent years and achieve promising effectiveness. In [25], the behind-the-meter distributed energy resources (DERs) are coordinated with the management of uncertainty to achieve collaborative distribution system restoration. In [26], the characteristics of high voltage direct current (HVDC) transmission systems are considered and a graph-theoretic-based parallel restoration method of AC-DC hybrid power systems is further proposed. In [27], a decision support framework is proposed as the coordination layer and partition optimization layer so as to achieve adaptive power system restoration.

Nevertheless, there still are research gaps between the existing methods and the actual power system restoration situations. The restoration characteristics of multiple types of loads, the network topology, the failure risk during restoration, and the interaction effects among multiple flexible resources (e.g., RES, EVS and ESS) are not cooperatively considered in detail during power system restoration in Refs. [5]–[24]. Concretely, restoration characteristics of multiple types of loads refer to the power consumption characteristics of different loads during restoration, and they can be modeled by constant load, ramping load, impulse load and flexible load. Failure risk refers to the failure possibility of a given scheme restoration due to unexpected issues (e.g., extreme weather and inherent faults), and it can be modeled by the recoverable rate of the lines to be restored. If these factors are neglected, then the load restoration process in the scheme as well as the success rate of the restoration scheme would be too optimistic when compared with reality. Therefore, a bi-level coordinated power system restoration (BiCPSR) model is proposed in this work considering the support of multiple flexible resources, restoration characteristics and network topology. The upper-level model aims to maximize the total generation capacity with the restoration failure possibility considered and to optimize the restoration path based on the network topology indices. The lower-level model aims to maximize the total restored load considering various scenarios and the support of multiple flexible resources. The contributions of this work are summarized as follows.

- 1) The restoration characteristics of multiple types of loads are further considered in the proposed model. Compared with the previous power system restoration models, the proposed model considers different characteristics of multiple types of loads (i.e., constant load, ramping load, impulse load and flexible load), the restoration of load in each bus is represented by piecewise linearization like the start-up characteristics of generators, which means the load restoration is more in line with the actual situation. Besides, case studies also show the advantages of considering the effectiveness of flexible load, which can accelerate the restoration and restore more load.

- 2) The start-up strategy of non-black-start generators, the restoration path, and the load restoration are considered coordinately in the proposed bi-level model, which can achieve a larger generation capacity and more restored load than most of the existing models. Besides, two network-topology indices are introduced to obtain a solid skeleton network during restoration, and the failure risk during restoration operation are also considered by the recoverable possibility of lines, which can help to characterize the influence of fault risks and achieve the higher recoverable rate of the final restoration scheme.
- 3) The support of multiple flexible resources for black-start and their regulation ability during power system restoration are considered in the proposed bi-level coordinated model, which can accelerate the restoration process. On the one hand, multiple flexible resources can help to provide additional black-start resources at the beginning of power system restoration; on the other hand, multiple flexible resources can help to mitigate the unbalance between load and power generation during the load restoration.

II. BI-LEVEL COORDINATED POWER SYSTEM RESTORATION MODEL

In this section, to form the bi-level power system restoration model, the start-up characteristics of generators, restoration characteristics of multiple types of loads and network-topology indices are represented, respectively. Then, the upper-level model is proposed for maximizing the total generation capacity with failure possibility and network-topology indices considered. Finally, the lower-level model is proposed for maximizing the total restored load with the support of multiple flexible resources considered.

A. Start-Up Characteristics of Generators and Restoration Characteristics of Multiple Types of Loads

The typical start-up characteristics of generators during power system restoration can be simplified as

$$P_{i,t}^{\text{start}} = \begin{cases} 0 & t < t_i^{\text{start}} \\ P_i^{\text{start}} & t \geq t_i^{\text{start}} \end{cases} \quad i \in \Omega_{\text{gen}} \quad (1)$$

$$P_{i,t}^{\text{gen}} = \begin{cases} 0 & t < t_i^{\text{R1}} \\ R_i(t - t_i^{\text{R1}}) & t_i^{\text{R1}} \leq t < t_i^{\text{R2}} \\ P_i^{\text{max}} & t \geq t_i^{\text{R2}} \end{cases} \quad i \in \Omega_{\text{gen}} \quad (2)$$

where Ω_{gen} is the set of generators. P_i^{start} , R_i and P_i^{max} are the nominal cranking power, ramping rate and maximum output of generator i , respectively. $P_{i,t}^{\text{start}}$ and $P_{i,t}^{\text{gen}}$ are the cranking power and output power of generator i at time t . t_i^{start} , t_i^{R1} and t_i^{R2} are the start-up time of generator i , the time that generator i begins to generate power and the time that the generated power of generator i reaches the maximum value, respectively. $T_i^{\text{R}} = t_i^{\text{R1}} - t_i^{\text{start}}$ is the required restoration time of generator i . The illustration of the start-up process of a generator is also given in Fig. 1. It is worth mentioning that the nominal cranking power (i.e., P_i^{start}) of black-start generators in power systems is ideally considered to be 0, since they can be self-restored.

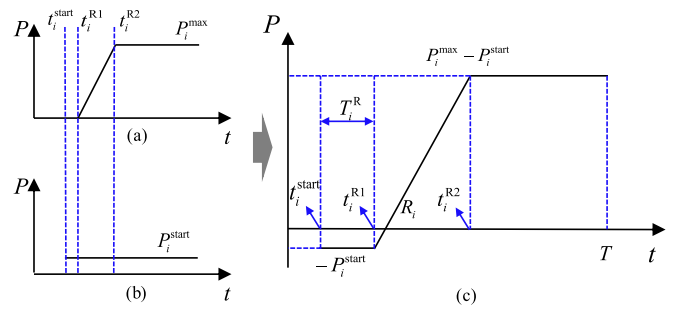


Fig. 1. Illustrations of start-up process of generators. (a) Generated power; (b) Cranking power; (c) Output power.

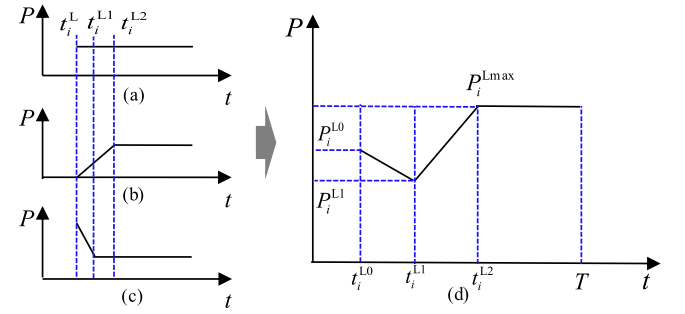


Fig. 2. Illustrations of the load restoration process. (a) Characteristic of constant load; (b) Characteristic of ramping load; (c) Characteristic of impulse load; (d) Characteristic of compound load.

In the past, the restoration characteristics of multiple types of loads $P_{i,t}^{\text{load}}$ are considered roughly. Concretely, it is either modeled as i) $0 \leq P_{i,t}^{\text{load}} \leq P_{i,t+1}^{\text{load}} \leq P_i^{\text{Lmax}}$, or ii) $P_{i,t}^{\text{load}} \in \{0, P_i^{\text{Lmax}}\}$ and $P_{i,t}^{\text{load}} \leq P_{i,t+1}^{\text{load}}$, where $P_{i,t}^{\text{load}}$ is the restored load of bus i at time t and P_i^{Lmax} is the original load before blackouts. In fact, the load restoration also has its inherent characteristics and some of them cannot be interrupted or jumped during the restoration process. For example, the load can be approximately divided as constant load, ramping load, impulse load and flexible load. Such classification and modeling can help the restoration scheme determined by the proposed model to be more in line with actual situations. The load restoration curves of the first three types are shown in Fig. 2. It can be seen that: i) Constant load has no relationship with the restoration process and its value keeps constants as the original value before blackouts once it is restored. In practice, the lighting load can be regarded as the typical constant load [28]. ii) Ramping load is quite small at the beginning of corresponding bus restoration and it needs a certain time to reach the rated value before blackouts. In practice, some small power substations or load aggregators can be regarded as the ramping load. It can also be regarded as an abstract basic element to form the compound load shown in Fig. 2(d). iii) Impulse load is quite large at the beginning of corresponding bus restoration and its value will decrease to the original value before blackouts after a certain time. In practice, the electric motor-related load and thermostatic controlled load can be regarded as the impulse load. Since cold load pickup (CLPU) refers to the phenomenon that automatic control loads including thermostatic controlled

loads start synchronously in the restoration process of the power system after a major power failure. In such a situation, the power value of load to be restored in the initial restoration period will be much greater than the steady-state load [29], [30]. Therefore, the cold load pickup characteristic can also be roughly represented by the impulse load. It is noted that this work mainly focuses on transmission network restoration and modeling the cold load pickup characteristic as impulse load is a trade-off between accuracy and computation efficiency.

Different from the traditional load that cannot be interrupted once it is restored, the flexible load can be shed again even if it has been restored in the previous restoration process, which is not considered for power system restoration in the past studies. In fact, such a feature of flexible load can help to accelerate the restoration process since it can make way for other critical loads and buses. To describe the new consideration of characteristics for the load during restoration, the following models are given.

$$P_{i,t}^{\text{load}} = \begin{cases} 0 & t < t_i^{L0} \\ \frac{P_i^{L1} - P_i^{L0}}{t_i^{L1} - t_i^{L0}} (t - t_i^{L0}) + P_i^{L0} & t_i^{L0} \leq t \leq t_i^{L1} \\ \frac{P_i^{L\max} - P_i^{L1}}{t_i^{L2} - t_i^{L1}} (t - t_i^{L1}) + P_i^{L1} & t_i^{L1} \leq t < t_i^{L2} \\ P_i^{L\max} & t \geq t_i^{L2} \end{cases} \quad i \in \Omega_{\text{bus}} - \Omega_{\text{FL}} \quad (3)$$

$$\begin{cases} P_{i,t}^{\text{load}} = 0 & t < t_i^{L0} \\ 0 \leq P_{i,t}^{\text{load}} \leq P_i^{L\max} & t \geq t_i^{L0} \end{cases} \quad i \in \Omega_{\text{FL}} \quad (4)$$

where t_i^{L0} , t_i^{L1} and t_i^{L2} are the time of bus i to be restored, the time that impulse load decreases to its rated value of bus i , and the time that ramping load increases to its rated value of bus i , respectively. t_i^{L0} is the variables to be optimized while t_i^{L1} and t_i^{L2} are inherent parameters related to the loads. In practice, t_i^{L1} and t_i^{L2} can be determined according to actual situations or estimated according to experience. P_i^{L0} and P_i^{L1} are the load of bus i at time t_i^{L0} and t_i^{L1} , respectively. Ω_{bus} and Ω_{FL} are the set of all buses and the set of the buses connected with the flexible load, respectively.

B. Network-Topology Indices

To obtain a solid skeleton network during the restoration process, two network-topology indices [31] measuring the bus importance are respectively introduced here. The network-topology indices for the k^{th} bus (i.e., reachability index I_k^{N1} and shortest reachable distance index I_k^{N2}) can be defined as

$$I_k^{\text{N1}} = \left(\sum_{i=1}^{N_{\text{bus}}} \sum_{j=1}^{N_{\text{bus}}} D_{ij}^{\text{N1}} - \sum_{i=1}^{N_{\text{bus}}} \sum_{j=1}^{N_{\text{bus}}} D_{ijk}^{\text{N1}'} \right) / 2 \quad (5)$$

$$I_k^{\text{N2}} = \left(\sum_i \sum_j D_{ijk}^{\text{N2}'} - \sum_i \sum_j D_{ijk}^{\text{N2}''} \right) / 2 \quad (i, j) \in \Omega_{\text{reach},k} \quad (6)$$

where N_{bus} is the number of buses in a given power system. D_{ij}^{N1} denotes whether bus i and bus j are reachable through the network, and $D_{ijk}^{\text{N1}'}$ denotes whether bus i and bus j are reachable through the network after removing bus k , respectively. They

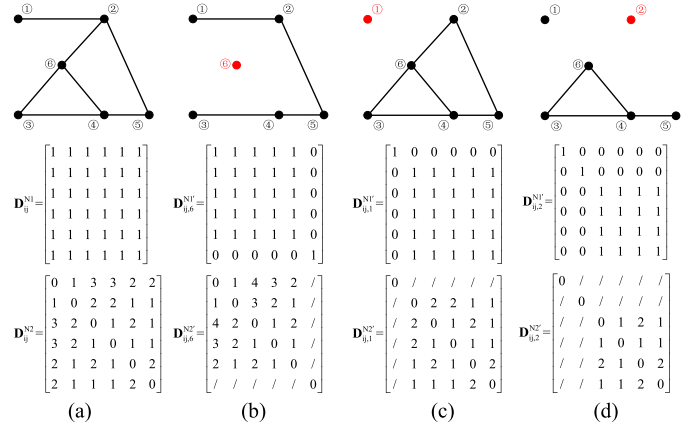


Fig. 3. Schematic diagram of network-topology indices measuring the node importance. (a) Original network; (b) Network after removing bus 6; (c) Network after removing bus 1; (d) Network after removing bus 2.

equal to 1 if the two buses are reachable; otherwise, they equal to 0. Therefore, the reachability index I_k^{N1} describes the topology connectivity loss after removing k . The larger the index is, the less the loss is, and the more important the bus k is. D_{ij}^{N2} denotes the shortest distance between bus i and bus j , and $D_{ijk}^{\text{N2}'}$ denotes the shortest distance between bus i and bus j after removing bus k , respectively. It is noted that the shortest distance between two buses in this work is determined as the number of lines in the shortest path between two buses. $\Omega_{\text{reach},k}$ is the set of reachable bus pairs after removing bus k . Therefore, the shortest reachable distance index I_k^{N2} describes the increased restoration time/cost after removing k . The larger the index is, the more the time/cost required for restoration, and the more important the bus k is. It is worth mentioning that the two network-topology indices represent the importance of a given bus in the original network. The more important the bus is, the higher priority it should be for restoration. In other words, the two indices of each bus can be determined before the blackout, therefore, they can still work even in a large-scale blackout.

To illustrate the two indices more clearly, an example with six buses is given in Fig. 3, and 3(a) shows the original network. In Fig. 3(b), bus 6 is removed from the original network: $I_6^{\text{N1}} = (36 - 26) / 2 = 5$, and $I_6^{\text{N2}} = (40 - 36) / 2 = 2$ since $\Omega_{\text{reach},6} = \{(1,2), (1,3), (1,4), (1,5), (2,3), (2,4), (2,5), (3,4), (3,5), (4,5), (2,1), (3,1), (4,1), (5,1), (3,2), (4,2), (5,2), (4,3), (5,3), (5,4)\}$. In Fig. 3(c), bus 1 is removed from the original network: $I_1^{\text{N1}} = (36 - 26) / 2 = 5$, and $I_1^{\text{N2}} = (28 - 28) / 2 = 0$ since $\Omega_{\text{reach},1} = \{(2,3), (2,4), (2,5), (2,6), (3,4), (3,5), (3,6), (4,5), (4,6), (5,6), (3,2), (4,2), (5,2), (6,2), (4,3), (5,3), (6,3), (5,4), (6,4), (6,5)\}$. In Fig. 3(d), bus 2 is removed from the original network: $I_2^{\text{N1}} = (36 - 18) / 2 = 9$, and $I_2^{\text{N2}} = (16 - 16) / 2 = 0$ since $\Omega_{\text{reach},2} = \{(3,4), (3,5), (3,6), (4,5), (4,6), (5,6), (4,3), (5,3), (6,3), (5,4), (6,4), (6,5)\}$. Since $I_2^{\text{N1}} + I_2^{\text{N2}} > I_6^{\text{N1}} + I_6^{\text{N2}} > I_1^{\text{N1}} + I_1^{\text{N2}}$, bus 2 is more important than bus 6, and bus 6 is more important than bus 1 in this example from the aspects of network-topology for restoration.

The index I_k^{N1} represents the influence of bus k on the reachability of different buses within the network, and the index I_k^{N2}

represents the influence of bus k on the overall connectivity of the network. Therefore, it can be seen that the two network-topology indices can measure the importance of buses in a given power system and can help to determine the skeleton network during the restoration process. The larger the values of the two indices are, the better the network topology is.

C. Optimal Generator Start-Up Strategy and Skeleton-Network Determination in the Upper-Level Model

As aforementioned, a solid skeleton network can contribute to the power system stability and reliability during restoration; besides, an appropriate generator start-up strategy can help to accelerate the process of load restoration in the lower level of the proposed model. Furthermore, during power system restoration, the recoverable rate of each transmission line which is influenced by the environment and weather factors, is different from the ones in the normal situation. Generally, during the black-start process and power system restoration, the recoverable rates of some lines would be quite low due to the potential faults and these increased failure risks should be considered in the power system model. Therefore, the initial objective function of the upper-level model that aims to find the optimal generator start-up strategy considering failure risks and to determine skeleton-network can be given as

$$\max \left[\sum_{i \in \Omega_{\text{gen}}} (E_i^{\text{gen}} - E_i^{\text{start}}) \prod_{l \in \Omega_{\text{res}}^L} \alpha_l + \sum_{i=1}^{N_{\text{bus}}} u_{i,T} I_i^{N1} + \sum_{i=1}^{N_{\text{bus}}} u_{i,T} I_i^{N2} \right] \quad (7)$$

where E_i^{gen} and E_i^{start} are the MW generation and cranking capabilities of generator i , Ω_{res}^L is the set of restored lines, α_l is the recoverable rate of the line l during restoration, respectively. T is the number of time steps during the restoration process and $u_{i,T}$ is a binary variable indicating the condition of bus i at time T . $u_{i,T} = 1$ if bus i is restored at time T and $u_{i,T} = 0$ otherwise. The first term of (7) denotes the total expected net output power capacity by generators with the recoverable rate considered. The second and third terms of (7) denote the values of two network-topology indices in the final restored network, respectively. Obviously, the larger the three terms of (7), the better the final restoration result. Therefore, (7) aims to maximize the total expected net output power capacity of generators and two network-topology indices. The impacts of extreme weather and other inherent uncertainties that would affect restoration success rate can be considered in the recoverable rate α_l . In this work, α_l are forecasted/assumed as given values in advance; however, they can be studied in details and set more elaborately by the methods in Refs. [19] and [32] as well. It has been demonstrated in [8], [19] that

$$\max \sum_{i \in \Omega_{\text{gen}}} (E_i^{\text{gen}} - E_i^{\text{start}}) \Leftrightarrow \min \sum_{i \in \Omega_{\text{gen}}} (P_i^{\text{max}} - P_i^{\text{start}}) t_i^{\text{start}} \quad (8)$$

$$\prod_{l \in \Omega_{\text{res}}^L} \alpha_l \approx 1 - \sum_{l \in \Omega_{\text{res}}^L} (1 - \alpha_l) \quad (9)$$

Therefore, (7) can be converted as

$$\min \left\{ - \sum_{i=1}^{N_{\text{bus}}} u_{i,T} I_i^{N1} - \sum_{i=1}^{N_{\text{bus}}} u_{i,T} I_i^{N2} + \sum_{i \in \Omega_{\text{gen}}} (P_i^{\text{max}} - P_i^{\text{start}}) t_i^{\text{start}} \left[1 - \sum_{l \in \Omega_{\text{res}}^L} (1 - \alpha_l) \right] \right\} \quad (10)$$

During the start-up process of generators and the determination of skeleton-network, several constraints should be satisfied as follows. As mentioned in Section II, the start-up characteristic of generators should be satisfied, and (1) and (2) can be linearized as

$$-(1 - z_{i,t})M \leq P_{i,t}^{\text{start}} \leq (1 - z_{i,t})M \quad (11)$$

$$-z_{i,t}M \leq P_{i,t}^{\text{start}} - P_i^{\text{start}} \leq z_{i,t}M \quad (12)$$

$$-z_{i,t}M \leq t - t_i^{\text{start}} \leq (1 - z_{i,t})M \quad (13)$$

$$-(1 - w_{i,t})M \leq P_{i,t}^{\text{gen}} \leq (1 - w_{i,t})M \quad (14)$$

$$-w_{i,t}M \leq P_{i,t}^{\text{gen}} - P_{i,t}^{\text{R1}} \leq w_{i,t}M \quad (15)$$

$$-w_{i,t}M \leq t - t_i^{\text{R1}} \leq (1 - w_{i,t})M \quad (16)$$

$$-(1 - v_{i,t})M \leq P_{i,t}^{\text{R2}} + P_i^{\text{max}} - R_i(t - t_i^{\text{R1}}) \leq (1 - v_{i,t})M \quad (17)$$

$$-v_{i,t}M \leq P_{i,t}^{\text{R2}} \leq v_{i,t}M \quad (18)$$

$$-v_{i,t}M \leq t - t_i^{\text{R2}} \leq (1 - v_{i,t})M \quad (19)$$

where M is a number large enough; $z_{i,t}$, $w_{i,t}$, and $v_{i,t}$ are 0-1 auxiliary variables for generator i at time t ; $P_{i,t}^{\text{R1}}$ and $P_{i,t}^{\text{R2}}$ are also corresponding auxiliary variables for generator i at time t . It is noted that introducing the auxiliary variable $z_{i,t}$ is aiming to convert (1) into (11)–(13) by the big-M method. It can be seen that: i) if $t < t_i^{\text{start}}$, then $z_{i,t} = 1$ according to (13) and $P_{i,t}^{\text{start}} = 0$ according to (11); ii) if $t > t_i^{\text{start}}$, then $z_{i,t} = 0$ according to (13) and $P_{i,t}^{\text{start}} = P_i^{\text{start}}$ according to (12). Therefore, (11)–(13) linearize the (1) by introducing the auxiliary variable $z_{i,t}$. Similarly, (14)–(19) linearize the (3) by introducing the auxiliary variables $w_{i,t}$, $v_{i,t}$, $P_{i,t}^{\text{R1}}$ and $P_{i,t}^{\text{R2}}$ as well. These auxiliary variables do not have physical meanings but help to linearize the nonlinear constraints.

In power systems, the generators to be started can be divided into the hot-start ones that should be started within a limited time, and the cold-start ones that cannot be started before a preparation time. Therefore, the constraint associated with the maximum/minimum critical start-up time of generators can be modeled as

$$T_i^{\text{Gmin}}/T_L \leq t_i^{\text{start}} \leq T_i^{\text{Gmax}}/T_L \quad i \in \Omega_{\text{gen}} \quad (20)$$

where T_L is the length of time step during the restoration process; and T_i^{Gmin} and T_i^{Gmax} are the maximum/minimum critical start-up time of generators, respectively. It is noted that t_i^{start} is a variable denoting the start time of generator i , and the lower and upper limits of constraints (20) respectively denote the earliest and the latest allowable start-up time for generator i .

The lines directly connected with the black-start generators cannot be restored until the black-start generators are restored. This constraint can be modeled as

$$\sum_{t=1}^T (1 - x_{l,t}) \geq t_i^{\text{start}} + T_i^{\text{R}}/T_L \quad i \in \Omega_{\text{BS}}, l \in \Omega_{\text{L_BS}} \quad (21)$$

where $x_{l,t}$ is a binary variable indicating the state of line l at time t . $x_{l,t} = 1$ if line l is restored at time t and $x_{l,t} = 0$ otherwise. Ω_{BS} and $\Omega_{\text{L_BS}}$ are the sets of black-start generators and the set of lines directly connected with black-start generators. Generally, the lines that have been restored should not be tripped again during the restoration process, therefore, this constraint is modeled as

$$0 \leq x_{l,t-1} \leq x_{l,t} \quad l \in \Omega_{\text{L}}, 1 \leq t-1, t \leq T \quad (22)$$

where Ω_{L} is the set of lines in the given power system. It is noted that buses, loads and non-black start generators also have similar rules during the restoration process. The rule for buses would be introduced in (27), and the rules for loads and non-black start generators have automatically been guaranteed by the sequential restoration constraints from (1) and (2), respectively.

The non-black-start generators can be restored only if the lines directly connected with them are restored in the previous time steps, and this requirement can be modeled as

$$\sum_{t=1}^T (1 - y_{i,t}) + 1 \leq t_i^{\text{start}} \quad i \in \Omega_{\text{NBS}} \quad (23)$$

$$x_{l,t} \leq y_{i,t} \quad i \in \Omega_{\text{NBS}}, l \in \Omega_{\text{L_NBS}} \quad (24)$$

$$y_{i,t} \leq \sum_{l \in \Omega_{\text{L_NBS}}} x_{l,t} \quad i \in \Omega_{\text{NBS}} \quad (25)$$

where $y_{i,t}$ is a binary variable indicating the condition of the non-black-start generator at bus i at time t . $y_{i,t} = 1$ if bus i is restored at time t and $y_{i,t} = 0$ otherwise. Ω_{NBS} and $\Omega_{\text{L_NBS}}$ are the sets of non-black-start generators and the set of lines directly connected with non-black-start generators.

For each line, it cannot be restored unless at least one adjacent line is restored or it is connected with a bus that has self-restoration ability (i.e., the bus connected with black-start generators, EVS, ESS, or RES). Generally, EVS and ESS have a certain black-start capacity [17], [18] since EVS would have several EVs and ESS would have a certain level of energy storage at any time. As for RES, its black-start capacity mainly depends on the weather situation. Concretely, solar power has no black-start capacity at night and wind power has no black-start capacity when the wind speed is too small or too large [16]. But anyway, whether they have black-start capacity can be known in advance and can be considered in the proposed power system restoration model according to the actual situations. Therefore, this constraint is modeled as

$$x_{l,t} \leq \sum_{k \in \Omega_{\text{L},l}} x_{k,t} \quad 1 \leq t-1, t \leq T$$

$$l \in \Omega_{\text{L}} - \Omega_{\text{L_BS}} - \Omega_{\text{L_EVS}} - \Omega_{\text{L_ESS}} - \Omega_{\text{L_RES}} \quad (26)$$

where $\Omega_{\text{L},l}$ is the set of lines that are directly connected with line l , and $\Omega_{\text{L_EVS}}$, $\Omega_{\text{L_ESS}}$ and $\Omega_{\text{L_RES}}$ are respectively the sets of lines

that are directly connected with black-start generator bus, EVS bus, ESS bus, and RES bus that can provide black-start ability in the actual situation before making restoration scheme.

In general, a bus can only be restored if at least one of the directly connected lines is restored and it cannot be outage again once it is restored. This constraint can be modeled as

$$0 \leq u_{i,t-1} \leq u_{i,t} \leq \sum_{l \in \Omega_{\text{L},i}} x_{l,t} \quad 1 \leq t-1, t \leq T \quad (27)$$

where $u_{i,t}$ is a binary variable indicating the condition of bus i at time t . $u_{i,t} = 1$ if bus i is restored at time t and $u_{i,t} = 0$ otherwise. $\Omega_{\text{L},i}$ is the set of lines that directly connected with bus i .

In summary, the upper-level model is

Objective function: (10)

Constraints: (11)–(27)

where $u_{i,t}$, $u_{i,T}$, $v_{i,t}$, $x_{l,t}$, $y_{i,t}$, $z_{i,t}$, $w_{i,t}$, $P_{i,t}^{\text{gen}}$, $P_{i,t}^{\text{start}}$, $P_{i,t}^{\text{start}}$, T_i^{R} , $P_{i,t}^{\text{R1}}$, $P_{i,t}^{\text{R2}}$, Ω_{RES} are state variables; and P_i^{start} , R_i , $P_{i,t}^{\text{max}}$, t_i^{R1} , t_i^{R2} , T_L , T_i^{Gmin} , T_i^{Gmix} , T_i^{N1} , T_i^{N2} , N_{bus} , M , α_l , Ω_{gen} , Ω_{bus} , Ω_{BS} , $\Omega_{\text{L},l}$, $\Omega_{\text{L},i}$, $\Omega_{\text{L_EVS}}$, $\Omega_{\text{L_ESS}}$, $\Omega_{\text{L_RES}}$ and $\Omega_{\text{L_BS}}$ are parameters that can be determined in advance.

D. Optimal Load Restoration Under Various Scenarios Associated With the Support of Multiple Flexible Resources in the Lower-Level Model

Load restoration is the ultimate aim of power system restoration. Furthermore, the uncertainties of flexible resources would result in the different performance of load restoration. Therefore, maximizing the load restoration under various scenarios associated with the support of multiple flexible resources is employed as the objective function of the lower-level model and it can be represented as

$$\max \sum_{s=1}^S \beta_s \sum_{i=1}^{N_{\text{bus}}} (\omega_i P_{i,T}^{\text{load}})_s \quad (28)$$

where S is the number of scenarios, β_s is the possibility of the s^{th} scenario. $P_{i,T}^{\text{load}}$ is the restored load at bus i at time T , and the subscript “ s ” denotes it is the corresponding value under the s^{th} scenario. ω_i is the parameter denoting the importance of load connected at bus i . The buses with critical infrastructure and services (e.g., hospitals and fire stations) [33], and load prioritization (e.g., high social burden and economic advantage) [34] should be given a larger ω_i . It should be worth mentioning that: i) The equations and constraints in Section II-D are discussed under the s^{th} scenario. For the convenience of formula derivation, the subscript “ s ” is omitted in the rest of Section II-D whenever no confusion arises. ii) The possibility β_s is obtained based on typical scenario generation and reduction with the actual data from Jianshan New District Zhejiang Province, China. More details can be found in the first part of Section III. iii) The more the number of scenarios, the more accurate the characterization of the uncertainty, the higher the computational burden.

As represented in Section II-A, the load restoration process has its inherent characteristics as modeled in equations (3), and

(3) can be reformulated as

$$P_{i,t}^{\text{load}} = u_{i,t}^{L0} \lambda_{1,i} + u_{i,t}^{L1} (\lambda_{2,i} - \lambda_{1,i}) + u_{i,t}^{L2} (P_i^{\text{Lmax}} - \lambda_{2,i} - \lambda_{1,i}) \quad (29)$$

where

$$u_{i,t}^{L0} = \begin{cases} 0 & t < t_i^{L0} \\ 1 & t \geq t_i^{L0} \end{cases} \quad u_{i,t}^{L1} = \begin{cases} 0 & t < t_i^{L1} \\ 1 & t \geq t_i^{L1} \end{cases} \quad u_{i,t}^{L2} = \begin{cases} 0 & t < t_i^{L2} \\ 1 & t \geq t_i^{L2} \end{cases} \quad (30)$$

$$\lambda_{1,i} = \frac{P_i^{L1} - P_i^{L0}}{t_i^{L1} - t_i^{L0}} (t - t_i^{L0}) + P_i^{L0},$$

$$\lambda_{2,i} = \frac{P_i^{\text{Lmax}} - P_i^{L1}}{t_i^{L2} - t_i^{L1}} (t - t_i^{L1}) + P_i^{L1} \quad (31)$$

Similar to the generator start-up characteristics, constraints (29)-(31) can be further converted into a linear form using big-M method [35], [36]. ESS can help to accelerate the process of power system restoration and its charge and discharge characteristics can be modeled as

$$0 \leq P_{i,t}^{\text{ESS}} \leq P_i^{\text{maxESSin}} \quad (32)$$

$$0 \leq P_{i,t}^{\text{ESSout}} \leq P_i^{\text{maxESSout}} \quad (33)$$

$$0 \leq E_{i,t}^{\text{ESS}} \leq E_i^{\text{maxESS}} \quad (34)$$

$$P_{i,t}^{\text{ESSin}} P_{i,t}^{\text{ESSout}} = 0 \quad (35)$$

$$E_{i,t}^{\text{ESS}} - E_{i,t-1}^{\text{ESS}} = \int_{t-1}^t (\eta_{\text{ESSin}} P_{i,t-1}^{\text{ESSin}} - \eta_{\text{ESSout}} P_{i,t-1}^{\text{ESSout}}) dt \quad (36)$$

where $P_{i,t}^{\text{ESSin}}$, $P_{i,t}^{\text{ESSout}}$ and $E_{i,t}^{\text{ESS}}$ are the input power, output power and remained energy of the ESS connected at bus i at time t , respectively. P_i^{maxESSin} , $P_i^{\text{maxESSout}}$, E_i^{maxESS} are the maximum input power, maximum output power, and nominal capacity of the ESS connected at bus i , respectively. η_{ESSin} and η_{ESSout} are the charge and discharge efficiency of the ESS, respectively. Constraints (35)-(36) can be further linearized as

$$-u_{i,t}^{\text{ESS}} M \leq P_{i,t}^{\text{ESSin}} \leq u_{i,t}^{\text{ESS}} M \quad (37)$$

$$-(1 - u_{i,t}^{\text{ESS}}) M \leq P_{i,t}^{\text{ESSout}} \leq u_{i,t}^{\text{ESS}} M \quad (38)$$

$$E_{i,t}^{\text{ESS}} - E_{i,t-1}^{\text{ESS}} = (\eta_{\text{ESSin}} P_{i,t-1}^{\text{ESSin}} - \eta_{\text{ESSout}} P_{i,t-1}^{\text{ESSout}}) \Delta t \quad (39)$$

where $u_{i,t}^{\text{ESS}}$ is the 0-1 auxiliary variable introduced for the linearization of ESS characteristics. Similar to ESS, EVS can also help to accelerate and support the power system restoration. The differences between ESS and EVS are that EVS is constituted by lots of vehicles while their user-behaviors are uncertain and should be considered. Thus, the characteristics of EVS are modeled as

$$0 \leq P_{i,n,t}^{\text{EVin}} \leq P_{i,n}^{\text{maxEVin}} \quad (40)$$

$$0 \leq P_{i,n,t}^{\text{EVout}} \leq P_{i,n}^{\text{maxEVout}} \quad (41)$$

$$0 \leq E_{i,n,t}^{\text{EV}} \leq E_{i,n}^{\text{maxEV}} \quad (42)$$

$$P_{i,t}^{\text{EVSin}} = \sum_{n=1}^{N_{i,t}^{\text{EV}}} P_{i,n,t}^{\text{EVin}} \quad (43)$$

$$P_{i,t}^{\text{EVSout}} = \sum_{n=1}^{N_{i,t}^{\text{EV}}} P_{i,n,t}^{\text{EVout}} \quad (44)$$

$$E_{i,n,t}^{\text{EV}} - E_{i,n,t-1}^{\text{EV}} = \int_{t-1}^t (\eta_{\text{EVin}} P_{i,n,t-1}^{\text{EVin}} - \eta_{\text{EVout}} P_{i,n,t-1}^{\text{EVout}}) dt \quad (45)$$

$$P_{i,n,t}^{\text{EVin}} P_{i,n,t}^{\text{EVout}} = 0 \quad (46)$$

where $P_{i,t}^{\text{EVSin}}$, $P_{i,t}^{\text{EVSout}}$ and $N_{i,t}^{\text{EV}}$ are the input power, output power, and number of EV of the EVS connected at bus i at time t , respectively. $E_{i,n}^{\text{maxEV}}$ is the nominal capacity of the n^{th} EV in the EVS connected at bus i . $P_{i,n,t}^{\text{EVin}}$, $P_{i,n,t}^{\text{EVout}}$ and $E_{i,n,t}^{\text{EV}}$ are the input power, output power and remained energy of the n^{th} EV in the EVS connected at bus i at time t , respectively. η_{EVin} and η_{EVout} are the charge and discharge efficiency of the EV, respectively. It should be mentioned that both the ESS and EVS in this work are infrastructures that are located in fixed places, and they are not mobile resources. Recently, some research has also studied the effectiveness of mobile resources (e.g., mobile emergency generators and mobile storage devices) with the corresponding pre-allocation problem, and more details can be found in [37]. In this work, the uncertainty of EVS is described by the uncertain number of EVs (i.e., $N_{i,t}^{\text{EV}}$), that is, different numbers of EVs in a given EVS before and during restoration would affect the black-start capability and power regulation ability of the EVS. Constraints (45)-(46) can be further linearized as

$$E_{i,n,t}^{\text{EV}} - E_{i,n,t-1}^{\text{EV}} = (\eta_{\text{EVin}} P_{i,n,t-1}^{\text{EVin}} - \eta_{\text{EVout}} P_{i,n,t-1}^{\text{EVout}}) \Delta t \quad (47)$$

$$-u_{i,n,t}^{\text{EV}} M \leq P_{i,n,t}^{\text{EVin}} \leq u_{i,n,t}^{\text{EV}} M \quad (48)$$

$$-(1 - u_{i,n,t}^{\text{EV}}) M \leq P_{i,n,t}^{\text{EVout}} \leq u_{i,n,t}^{\text{EV}} M \quad (49)$$

where $u_{i,n,t}^{\text{EV}}$ is the 0-1 auxiliary variable introduced for the linearization of EV characteristics. Finally, the power balance constraints should be satisfied as

$$\sum_{i \in \Omega_{\text{gen}}} (P_{i,t}^{\text{gen}} - P_{i,t}^{\text{start}}) + \sum_{i \in \Omega_{\text{EVS}}} (P_{i,t}^{\text{EVSout}} - P_{i,t}^{\text{EVSin}}) + \sum_{i \in \Omega_{\text{ESS}}} (P_{i,t}^{\text{ESSout}} - P_{i,t}^{\text{ESSin}}) + \sum_{i \in \Omega_{\text{PV}}} P_{i,t}^{\text{PV}} + \sum_{i \in \Omega_{\text{WD}}} P_{i,t}^{\text{WD}} \geq 0 \quad (50)$$

$$\sum_{l \in \Omega_{L,i}} P_{l,t} = P_{i,t}^{\text{gen}} + P_{i,t}^{\text{PV}} + P_{i,t}^{\text{WD}} - P_{i,t}^{\text{start}} - P_{i,t}^{\text{load}} + P_{i,t}^{\text{EVSout}} - P_{i,t}^{\text{EVSin}} + P_{i,t}^{\text{ESSout}} - P_{i,t}^{\text{ESSin}} \quad (51)$$

where $P_{i,t}^{\text{PV}}$ and $P_{i,t}^{\text{WD}}$ are the output of solar and wind generation at bus i at time t , respectively. $P_{l,t}$ is the power flow through the line l . Ω_{ESS} , Ω_{EVS} , Ω_{PV} and Ω_{WD} are the sets of ESS, EVS, solar power and wind power, respectively. In (50) and (51), it can be seen that the EVS, ESS and RES can provide more flexible

resources for balancing the power generation and consumption during power system restoration, which means it would be more possible to achieve power balance and further accelerate the restoration process when considering these multiple flexible resources.

In summary, the lower-level model is

Objective function: (28)

Constraints: (29)–(34), (37)–(44), (47)–(51) $\forall s$ where $P_{i,T}^{\text{load}}, P_{i,t}^{\text{EVsin}}, P_{i,t}^{\text{EVsout}}, P_{i,n,t}^{\text{EV in}}, P_{i,n,t}^{\text{EV out}}, P_{l,t}, E_{i,t}^{\text{ESS}}, E_{i,n,t}^{\text{EV}}, u_{i,t}^{\text{ESSin}}$, and $u_{i,n,t}^{\text{EV}}$ are state variables; $P_i^{\text{maxESSin}}, P_i^{\text{maxESSout}}, E_i^{\text{maxESS}}, E_{i,n}^{\text{maxEV}}, \eta_{\text{ESSin}}, \eta_{\text{ESSout}}, \eta_{\text{EVin}}, \eta_{\text{EVout}}, \Omega_{\text{ESS}}, \Omega_{\text{EVS}}, \Omega_{\text{PV}}$ and Ω_{WD} are parameters that can be determined in advance, respectively. It should be mentioned that $N_{i,t}^{\text{EV}}, P_{i,t}^{\text{PV}}$ and $P_{i,t}^{\text{WD}}$ are uncertain variables and they would vary with different scenarios and characterize the fluctuant and intermittent natures of wind and solar power. At present, the methods to deal with uncertain variables mainly include: i) stochastic optimization, ii) chance-constrained programming, iii) robust optimization, and iv) scenario analysis. In this work, the uncertainties are considered by various power output scenarios of RES and various scenarios for different numbers of EVs in EVS. Through scenario analysis, the uncertainly programming with uncertain variables (i.e., the fluctuant and intermittent natures of wind and solar power) can be converted into normal MILP with different typical scenarios. More details can be found in Section III.

It should be noted that the branch flow, frequency, and voltage constraints should also be considered and would be checked for each generated restoration scheme. Besides, solutions from DC power flow model-based restoration models can be infeasible with respect to AC power flow model. However, it is hard to consider AC power flow constraints indeed during restoration for the transmission network. Therefore, the AC feasibility would also be satisfied by checking for each potential generated restoration scheme in practice. In fact, the proposed model can obtain several potential best or second-best solutions, and the final scheme is determined as the first solution that can pass the checkout.

III. CASE STUDIES

To show the effectiveness of the proposed power system restoration model, the revised IEEE 39-bus and WECC 179-bus systems, and the actual Zhejiang power systems of China are employed respectively for demonstration, and the results obtained by other power system restoration models are also given for comparisons. For the three power systems, they are all assumed in the complete outage situation before restoration, i.e., all lines and buses are disconnected and in an outage. In this section, 2:00, 10:00 and 18:00 are selected as the start time of restoration to simulate the midnight, morning, and dusk times. Therefore, these three typical times are selected in this work while it does not matter to select other suitable times to study.

The typical curves of wind power and solar power outputs are obtained based on the actual data from Jianshan New District Zhejiang Province, China [38] (also can be obtained based on other actual databases such as [39]). Concretely, the wind

TABLE I
SEVERAL PARAMETERS OF THE REVISED IEEE 39-BUS AND THE REVISED WECC 179-BUS SYSTEM

Parameter	Value	Parameter	Value	Parameter	Value
T_L	5min	η_{ESSin}	95%	η_{ESSout}	95%
P_i^{maxESSin}	1 pu	η_{EVin}	95%	η_{EVout}	95%
$P_i^{\text{maxESSout}}$	1 pu	E_i^{maxESS}	1 pu	$E_{i,n}^{\text{maxEV}}$	1 pu
P_i^{maxEVin}	10^{-4} pu	P_i^{maxEVout}	10^{-4} pu		

and solar power data of one year (i.e., 365 daily curves) are utilized to generate the typical wind and solar curves based on k-means clustering. Then, 6 typical scenarios, i.e., spring sunny day (23.4%), summer sunny day (24.1%), autumn sunny day (13.1%), winter sunny day (13.1%), cloudy day (20.4%), and rainy day (5.9%) for solar; and 3 typical scenarios, i.e., high speed (13.1%), middle speed (23.1%), and low speed (63.8%), for wind can be obtained. The final scenarios and corresponding possibility β_s are determined by the combination of them. Besides, for both the revised power system and the revised WECC 179-bus system, some parameters are set and shown in Table I.

It is noted that the rest parameters (i.e., $t_i^{\text{R1}}, t_i^{\text{R2}}, I_i^{\text{N1}}, I_i^{\text{N2}}, N_{\text{bus}}, M, \alpha_l, \Omega_{\text{gen}}, \Omega_{\text{bus}}, \Omega_{\text{BS}}, \Omega_{L,l}, \Omega_{L,i}, \Omega_{L,\text{EVS}}, \Omega_{L,\text{ESS}}, \Omega_{L,\text{RES}}, \Omega_{L,\text{BS}}, \Omega_{\text{ESS}}, \Omega_{\text{EVS}}, \Omega_{\text{PV}}$ and Ω_{WD}) involved in the power restoration model for the revised IEEE 39-bus and WECC 179-bus system can be either obtained from [40], [41] or determined by the above given parameters.

A. Case Studies and Comparisons in the Revised IEEE 39-Bus System

As one of the well-known power systems, the IEEE 39-bus system is used for illustrating the proposed power system model and the detailed electrical parameters of IEEE 39-bus system can be found in [40]. On this basis, it is assumed that a wind power plant, a PV power plant, an ESS and an EVS are deployed in Bus 3, Bus 23, Bus 5 and Bus 15, respectively. The black-start generator is assumed to be deployed in Bus 30. Besides, it is assumed that the recoverable rate of the line from Bus 5 to Bus 6 is 50% and the ones of all other lines are 99.9% to simulate the practical situation after blackouts due to extreme weather or destruction. Thus, the revised IEEE 39-bus system is shown in Fig. 4 and the restoration path is determined as shown in Table II.

It can be seen from Table II that: i) For Case 1, the system restoration starts at the buses connected with the wind power plant, ESS and EVS. ii) For both Case 2 and Case 3, the system restoration starts at the buses connected with the wind power plant, solar power plant, ESS and EVS. iii) For all three cases, the black-start generator begins to restore other buses after a certain time period. iv) All the restoration paths of the three cases do not include the line from Bus 5 to Bus 6. The reasons for these phenomena can be summarized as: i) The solar power plant cannot support the power system restoration in Case 1 since this case is at midnight and the solar power plant has no output. ii) Correspondingly, Case 2 and Case 3 are in the daytime, which means the solar power plant can provide strong support for the restoration. iii) Although the black-start generator has the self-restored ability, it requires a certain time to generate power

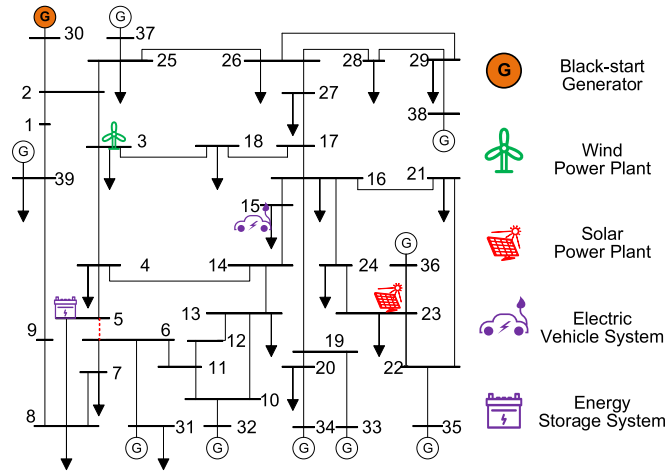


Fig. 4. Schematic diagram of the revised IEEE 39-bus system.

TABLE II
RESTORATION PATH DETERMINED BY THE PROPOSED MODEL IN THE REVISED IEEE 39-BUS SYSTEM

	Case 1	Case 2	Case 3
<i>t</i>	Path	<i>t</i>	Path
5	3→2, 5→8, 15→14, 15→16, 23→22, 23→36	5	3→2, 5→4, 5→8, 15→16, 23→22, 23→36
10	2→25, 8→7, 14→13, 22→35	10	2→25, 4→14, 22→35
15	7→6, 13→10, 16→19, 25→37, 25→26	15	2→1, 8→7, 14→13, 16→19, 25→26, 25→37
20	19→20, 26→29	20	7→6, 13→10, 19→20, 26→29
25	6→31, 10→32, 20→34, 29→38	25	6→31, 10→32, 16→24, 20→34, 29→38
30	2→1	30	1→39
35	1→39	60	19→33
60	16→24	65	26→27
65	19→33	105	16→21
75	14→4		
125	26→27		
135	16→21		

Note: The unit for *t* is minute.

for supply, which means it cannot restore the power system immediately. iv) The proposed model considers the recoverable rate of different restoration schemes, which means the schemes containing restoring lines with low recoverable rates would be abandoned.

The results of power system restorations that begin at 2:00 (Case 1), 10:00 (Case 2) and 18:00 (Case 3) are respectively given in Fig. 5 and Table III, and the results obtained by other models are also given in Fig. 5 and Table III for comparisons.

It can be seen from Fig. 5 and Table III that the proposed BiCPSR model can always achieve the best performance than other models (i.e., the largest values for generation capacity,

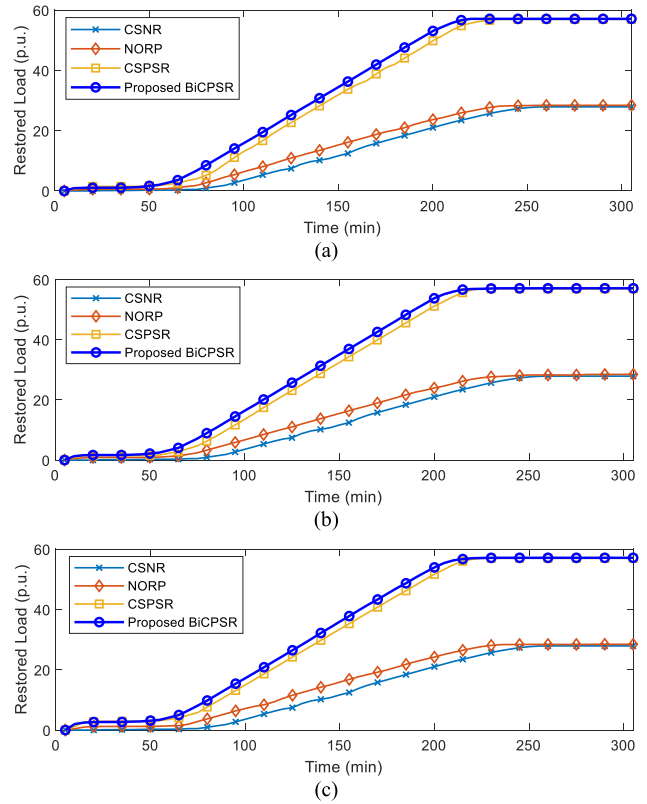


Fig. 5. Restoration processes of Case 1, Case2 and Case 3 in the revised IEEE 39-bus system. (a) Case 1; (b) Case 2; (c) Case 3.

recoverable rate, expected restored load and network topology). For the generation capacity, the multiple flexible resources are considered together and utilized for black-start in the proposed model. Therefore, the proposed model obtains the largest generation capacity for all three cases.

For the recoverable rate, the line from Bus 5 to Bus 6 is expected to be restored by the CSNR [13] and NORP [16] models. However, this line is with a low recoverable rate in the previous assumption. Therefore their final recoverable rate is also quite low. The CSPSR model [19] and the proposed BiCPSR model can consider the impact of the recoverable rate of equipment during the restoration process, so they avoid trying to restore line from Bus 5 to Bus 6 and can obtain a high recoverable rate. The reason for the slightly higher recoverable rate of the proposed model when compared with the CSPSR model [19] is that the proposed model chooses a better restoration path to avoid unnecessary operations during restoration.

For the expected restored load, CSNR [13] and NORP [16] models obtain the lower value due to the same reason (i.e., they cannot consider the recoverable rate of equipment during restoration). Besides, the proposed model can achieve a larger expected restored load than the one of the CSPSR model [19] since the proposed model further considers the effectiveness of PV, ESS and EVS (CSPSR model [19] just considers the wind power generation), which can provide additional power for load restoration. For the same reason, the RES (including solar and wind power), ESS and EVS can also be regarded as the

TABLE III
COMPARISONS BETWEEN THE PROPOSED MODEL AND THE OTHER
STATE-OF-THE-ART MODELS IN THE REVISED IEEE 39-BUS SYSTEM

Case	Models	Generation Capacity (p.u.)	Recoverable Rate	Expected Restored Load (p.u.)	Network Topology
1 (2:00 in the day)	CSNR	2680.42	45.767%	28.410	7.5123
	NORP	2524.51	45.600%	27.904	7.5712
	CSPSR	2667.58	96.900%	56.931	6.8700
	Proposed BICPSR	2747.46	97.200%	57.107	10.7226
2 (10:00 in the day)	CSNR	2680.42	45.733%	28.485	7.5712
	NORP	2524.51	45.600%	27.904	7.5712
	CSPSR	2667.58	96.900%	56.931	6.8700
	Proposed BICPSR	2747.46	97.200%	57.107	10.8314
3 (18:00 in the day)	CSNR	2680.42	45.667%	28.442	7.5712
	NORP	2524.51	45.600%	27.904	7.5712
	CSPSR	2667.58	96.900%	56.931	6.8700
	Proposed BICPSR	2747.46	97.200%	57.107	10.8096

CSNR: Comprehensive Skeleton-Network Restoration [13]

NORP: Novel Offline Restoration Planning [16]

CSPSR: Case-Sensitive Power System Restoration [19]

black-start resources at the beginning of system restoration and can help to accelerate the restoration process. It is noted that the restoration actions are finished at 135min, 105min and 130min in Table II, while the restored load continuously increases until around the 210min in Fig. 5. The reason is that although buses and lines are restored, the generators require a certain time to ramp to their maximum output so as to restore more loads. Therefore, there would be a certain delay for the load restoration in Fig. 5.

For the network topology, it can be seen that the proposed model also achieves the highest value since it can determine a more suitable restoration path to reconfigure the skeleton network.

It can be seen from Table III that the results of the proposed model for different cases are also different. The reason is that the conditions of RES, ESS and EVS vary with time. For example, there is no solar power generation in Case 1 since this case begins at 2:00. Therefore, solar power cannot help the power system restoration for this case and the time step required for restoration is longer than Case 2 and Case 3. Similarly, the wind power generation is different for the three cases, so the results obtained by the NORP [16] and CSPSR [19] models, which consider wind power generation, are also different. For the CSNR [13], it does not consider flexible resources, therefore, the results of all three cases are the same.

B. Case Studies and Comparisons in the Revised WECC 179-Bus System

For demonstrating the effectiveness of the proposed power system restoration model in bulk power systems and considering the power system restoration resources with multi black-start generators, multi EVS, multi ESS and multi RES, the revised

TABLE IV
RESTORATION PATH DETERMINED BY THE PROPOSED MODEL IN THE REVISED
WECC 179-BUS SYSTEM

t	Case 4	Case 5	Case 6
5	25→13, 25→26, 80→98, 80→179	25→13, 25→26, 80→98, 80→179	25→13, 25→26, 80→98, 80→179
10	13→28, 26→138, 179→85	13→28, 26→138, 98→83, 179→85	13→28, 26→138, 98→83, 179→85
15	27→28, 138→63, 85→87, 138→141, 138→137	138→11, 27→28, 138→63, 85→87, 138→141, 138→146, 83→84, 138→137	27→28, 138→63, 85→87, 138→141, 83→84, 138→137
...
65	32→33, 116→100, 116→115	32→33, 116→100, 116→115	32→33, 116→100, 11→12, 116→115
70	100→112, 11→12, 33→34	100→112, 33→34	100→112, 33→34
75	112→111	112→111	112→111

Note: The unit for t is minute.

WECC 179-bus system is also employed in this work for case studies.

The WECC 179-bus system is the simplification of the actual western electricity coordinating council (WECC) power system, whose detailed parameters can be found in [41]. On this basis, it is assumed that one wind power plant is deployed in Bus 3, one PV power plant is deployed in Bus 24, two ESS are deployed in Bus 25 and Bus 32, and two EVS are deployed in Bus 10 and Bus 53, respectively. The black-start generators are assumed to be deployed in Bus 15, Bus 36 and Bus 43, respectively. Besides, it is assumed that the recoverable rates of the line from Bus 14 to Bus 21 is 50% and the ones of all other lines are 99.9% to simulate the practical situation after blackouts due to extreme weather or destruction.

Thus, the restoration path is determined as shown in Table IV. It can be seen from Table IV that similar phenomena with the revised IEEE 39-bus systems can be observed and multi-power system restoration resources can help to restore the power system parallelly and accelerate the restoration process. Since it is assumed that the line between Bus 14 and Bus 21 is with a low recoverable rate (i.e., 50%), this line is not restored in the restoration schemes for Cases 4-6 determined by the proposed model.

The results of power system restorations that begin at 2:00 (Case 4), 10:00 (Case 5) and 18:00 (Case 6) are respectively given in Fig. 6 and Table V, and the results obtained by other models are also given in Fig. 6 and Table V for comparisons. It can be seen that the proposed power system restoration model can achieve better performance than other models for most of the indices.

For the generation capacity, the multiple flexible resources can help to crank the non-black start generators more rapidly, so the proposed model can always obtain the largest values. For the recoverable rate and expected restored load, the proposed model can consider the recoverable rate of the transmission line so as to achieve good performance and be more suitable for practical situations. For network-topology indices, the proposed model

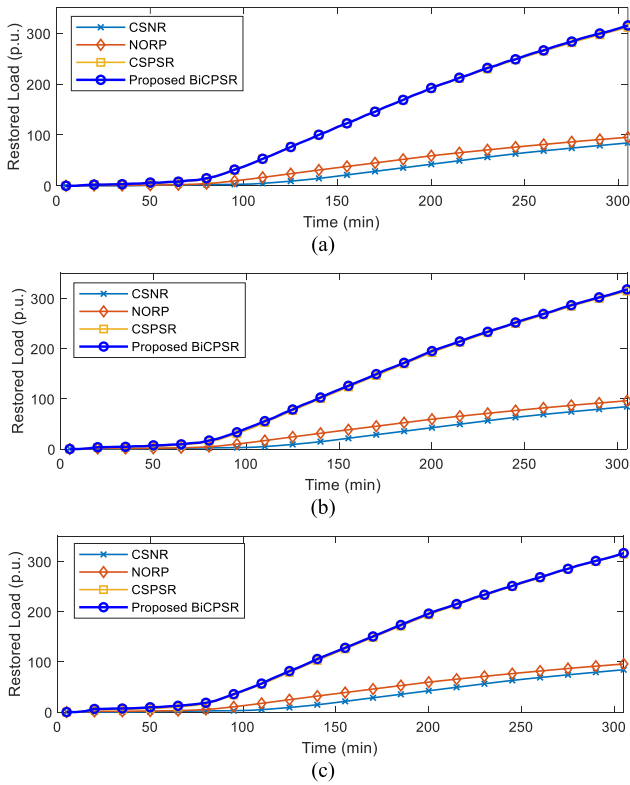


Fig. 6. Restoration processes of Case 4, Case 5 and Case 6 in the revised WECC 179-bus system. (a) Case 4; (b) Case 5; (c) Case 6.

TABLE V
COMPARISONS BETWEEN THE PROPOSED MODEL AND THE OTHER STATE-OF-THE-ART MODELS IN THE REVISED WECC 179-BUS SYSTEM

Case	Models	Generation Capacity (p.u.)	Recoverable Rate	Expected Restored Load (p.u.)	Network Topology
4 (2:00 in the day)	CSNR	4683.64	27.900%	84.295	8.1844
	NORP	5963.78	27.900%	95.475	10.1939
	CSPSR	19517.54	91.633%	313.369	6.8483
	Proposed BiCPSR	19520.20	91.500%	314.946	11.4975
5 (10:00 in the day)	CSNR	4683.64	27.900%	84.295	8.1844
	NORP	5963.78	27.900%	96.051	9.3802
	CSPSR	19503.63	91.433%	314.778	6.8897
	Proposed BiCPSR	19518.44	91.500%	317.770	11.4975
6 (18:00 in the day)	CSNR	4683.64	27.900%	84.295	8.1844
	NORP	5963.78	27.900%	95.798	10.2402
	CSPSR	19496.55	91.433%	313.948	6.8686
	Proposed BiCPSR	19518.44	91.500%	316.523	11.4975

also can achieve the largest values, whose reason is similar to the cases in the revised IEEE 39-bus system. Therefore, it can be concluded that the proposed model can obtain good performance in bulk power systems and is adapted to practical situations.

TABLE VI
COMPARISONS BETWEEN THE PROPOSED MODEL AND THE OTHER STATE-OF-THE-ART MODELS IN THE ACTUAL ZHEJIANG POWER SYSTEM

Case	Models	Generation Capacity (p.u.)	Recoverable Rate	Expected Restored Load (p.u.)	Network Topology
7 (2:00 in the day)	CSNR	15316.50	40.200%	99.387	13.9176
	NORP	17163.29	40.200%	108.378	14.1170
	CSPSR	17137.76	95.400%	257.195	15.8376
	Proposed BiCPSR	17153.64	95.400%	261.488	20.6317
8 (10:00 in the day)	CSNR	15316.50	40.200%	99.387	13.9176
	NORP	17164.35	40.200%	108.793	12.1432
	CSPSR	17137.76	95.400%	258.181	15.6046
	Proposed BiCPSR	17162.56	95.400%	262.960	20.6317
9 (18:00 in the day)	CSNR	15316.50	40.200%	99.387	13.9176
	NORP	17167.29	40.200%	108.611	12.9950
	CSPSR	17137.76	95.400%	257.748	15.8928
	Proposed BiCPSR	17564.53	95.400%	262.310	20.6317

C. Case Studies and Comparisons in the Actual Zhejiang Power System of China

To illustrate the feasibility of the proposed BiCPSR model, the simplified version of the actual Zhejiang power system of China is utilized for demonstration. In this power system, there are 83 buses in total, and three of them are with 1000kV-level and eighty of them are with 500kV-level. There are eighteen power plants including thermal power, nuclear power and pump storage ones. Besides, the power from other provinces is also simplified as seven equivalent buses. For power system restoration, pump storage plants are usually utilized as the black-start generators, therefore, the three pump storage plants at Bus 30, Bus 73 and Bus 76 are regarded as the black-start generators. Besides, two ESSs are deployed at Bus 28 and Bus 44, one PV power plant is installed at Bus 57, one wind power plant is installed at Bus 23, one EVS is installed at Bus 12, respectively. Furthermore, it is assumed that the recoverable rates of the line from Bus 32 to Bus 33 is 50% and the ones of all other lines are 99.9% to simulate the practical situation after blackouts due to extreme weather or destruction. The results of power system restorations that begin at 2:00 (Case 7), 10:00 (Case 8) and 18:00 (Case 9) are respectively given in Table VI. It can be seen that the proposed BiCPSR model achieves the largest values of the recoverable rate (i.e., 95.400%), expected restored load (i.e., 261.488MW, 262.960MW and 262.310MW) and network topology (i.e., 20.6317) for Cases 7-9. For the generation capacity, the values achieved by the proposed BiCPSR model are slightly smaller than the ones of the NORP model [16]. However, the recoverable rate is not considered in the NORP model, which means that one of the steps (i.e., restoring the line from Bus 32 to Bus 33) of the NORP model for Cases 7-9 may fail. In fact, if the expected values of generation capacity are utilized for comparison, the expected values of the NORP model would decrease sharply.

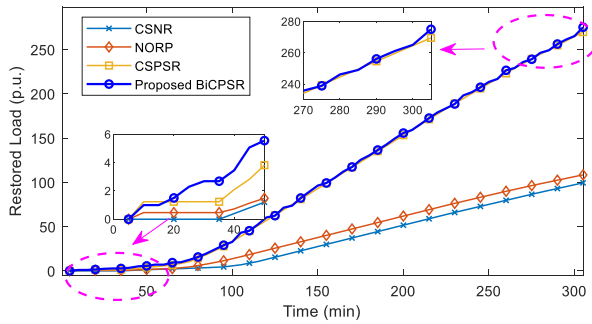


Fig. 7. Restoration processes of Case 9 in the actual Zhejiang power system.

To show the restoration process more clearly, the detailed view for Case 9 is given in Fig. 7, and two zoom-in views are plotted for the beginning and the ending of the system restoration. It can be seen that the CSNR model [13] restores the load slower than the other three models, the reason is that it does not consider the effectiveness of wind power generation for black-start. Accordingly, the proposed BiCPSR model can restore the load faster than the other three models at the beginning of the restoration, and the reason is that it further considers the effectiveness of solar power generation, EVS and ESS for black-start. Similarly, it can be seen from the second zoom-in view that the proposed BiCPSR model can restore the most load when compared with the other three models. Therefore, it can be concluded that the proposed BiCPSR model is better than the other three ones.

D. Discussions for the Proposed BiCPSR Model

It can be seen from Cases 1-9 that the proposed BiCPSR model outperforms other models from all four aspects. In particular, compared with the CSPSR model [19], the proposed BiCPSR model further considers the coordination effectiveness of solar power generation, ESS and EVS. Therefore, the proposed BiCPSR model can achieve a better performance than the CSPSR model [19] w.r.t. the generation capacity and expected restored load. Besides, the proposed BiCPSR model also considers the network-topology indices, so it can obtain a more suitable skeleton network when compared with the CSPSR model [19].

To illustrate the advantages of considering flexible load in the power system restoration, the restoration processes for Case 9 with and without flexible load considered are shown in Fig. 8. It can be seen that the load restored would increase continuously if the flexible load is not considered, which is required by the constraint that restored load cannot be shed again. However, if the flexible load is considered, then the load restored may decrease for a certain period (e.g., the 55min~60min in Fig. 8), which means that some restored load is shed again. In the meantime, however, the surplus power generation would help to restore more critical lines and buses so as to restore more load in near future. In fact, as the saying goes, more preparation may quicken the speed in doing work. It can be seen from the right part of Fig. 8 that the restoration process considering flexible load achieves more load restoration than the ones without considering flexible load.

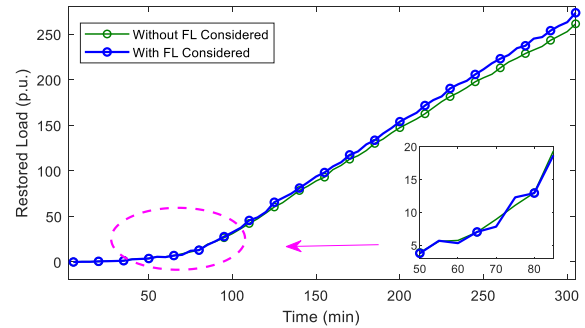


Fig. 8. Restoration processes of Case 9 in the actual Zhejiang power system with and without the flexible load considered.

IV. CONCLUSION

In this work, a bi-level coordinated power system restoration model considering the support of multiple flexible resources is proposed. The proposed model considers the whole three stages (i.e., black-start zone partitioning, network reconfiguration and load restoration) together [2] with $T_L = 5$ min operation action interval and the whole restoration would take several hours. Although the model is a little complex, it is still feasible in practice. In the upper-level model, two network-topology indices are proposed for searching the skeleton network during restoration and the generator start-up sequences are determined with aim of maximizing total generation capacity. In the lower level, the support of multiple flexible resources is considered comprehensively and typical scenarios are utilized to describe their uncertainties of them. Besides, the restoration characteristics of multiple types of loads are first considered and the recoverable rates of transmission lines during the restoration process are considered, which makes the obtained restoration scheme more in line with the actual situations. Therefore, compared with the state-of-the-art models, the proposed model can achieve better performance regarding generation capacity, recoverable rate, expected restored load, and network topology. This work mainly focuses on the framework to consider the three stages of power system restoration together, while some specific details are not explored. To study how to further develop the pre-allocation of black-start resources [33], the importance of load associated with critical infrastructure, services and corresponding economic consequences [34] in the model, and how to develop the detailed relationship between recoverable rate and extreme weather [32] are our research directions in the future.

REFERENCES

- [1] S. Liu *et al.*, "Data-driven event identification in the U.S. power systems based on 2D-OLPP and RUSBoosted trees," *IEEE Trans. Power Syst.*, vol. 37, no. 1, pp. 94–105, Jan. 2022.
- [2] F. Qiu and P. Li, "An integrated approach for power system restoration planning," *Proc. IEEE*, vol. 105, no. 7, pp. 1234–1252, Jul. 2017.
- [3] Y. Liu, R. Fan, and V. Terzija, "Power system restoration: A literature review from 2006 to 2016," *J. Modern Power Syst. Clean Energy*, vol. 4, no. 3, pp. 332–341, Jul. 2016.
- [4] S. Liu *et al.*, "Robust system separation strategy considering online wide-area coherency identification and uncertainties of renewable energy sources," *IEEE Trans. Power Syst.*, vol. 35, no. 5, pp. 3574–3587, Sep. 2020.

- [5] Z. Z. Lin, F. S. Wen, C. Y. Chung, K. P. Wong, and H. Zhou, "Division algorithm and interconnection strategy of restoration subsystems based on complex network theory," *IET Gener., Transmiss. Distrib.*, vol. 5, no. 6, pp. 674–683, Jun. 2011.
- [6] C. Wang, V. Vittal, and K. Sun, "OBDD-based sectionalizing strategies for parallel power system restoration," *IEEE Trans. Power Syst.*, vol. 26, no. 3, pp. 1426–1433, Aug. 2011.
- [7] L. Sun *et al.*, "Network partitioning strategy for parallel power system restoration," *IET Gener., Transmiss. Distrib.*, vol. 10, no. 8, pp. 1883–1892, Apr. 2016.
- [8] W. Sun, C. Liu, and L. Zhang, "Optimal generator start-up strategy for bulk power system restoration," *IEEE Trans. Power Syst.*, vol. 26, no. 3, pp. 1357–1366, Aug. 2011.
- [9] Y. Jiang and T. H. Ortmeier, "Propagation-based network partitioning strategies for parallel power system restoration with variable renewable generation resources," *IEEE Access*, vol. 9, pp. 144965–144975, 2021.
- [10] B. Chen, C. Chen, J. Wang, and K. L. Butler-Purry, "Multi-time step service restoration for advanced distribution systems and microgrids," *IEEE Trans. Smart Grid*, vol. 9, no. 6, pp. 6793–6805, Nov. 2018.
- [11] S. Abbasi, M. Barati, and G. J. Lim, "A parallel sectionalized restoration scheme for resilient smart grid systems," *IEEE Trans. Smart Grid*, vol. 10, no. 2, pp. 1660–1670, Mar. 2019.
- [12] A. Golshani, W. Sun, and K. Sun, "Advanced power system partitioning method for fast and reliable restoration: Toward a self-healing power grid," *IET Gener., Transmiss. Distrib.*, vol. 12, no. 1, pp. 42–52, Jan. 2018.
- [13] L. Sun, Z. Lin, Y. Xu, F. Wen, C. Zhang, and Y. Xue, "Optimal skeleton-network restoration considering generator start-up sequence and load pickup," *IEEE Trans. Smart Grid*, vol. 10, no. 3, pp. 3174–3185, May 2019.
- [14] X. Gu, G. Zhou, S. Li, and T. Liu, "Global optimisation model and algorithm for unit restarting sequence considering black-start zone partitioning," *IET Gener., Transmiss. Distrib.*, vol. 13, no. 13, pp. 2652–2663, Jul. 2019.
- [15] A. M. El-Zonkoly, "Renewable energy sources for complete optimal power system black-start restoration," *IET Gener., Transmiss. Distrib.*, vol. 9, no. 6, pp. 531–539, Mar. 2015.
- [16] A. Golshani, W. Sun, Q. Zhou, Q. P. Zheng, and Y. Hou, "Incorporating wind energy in power system restoration planning," *IEEE Trans. Smart Grid*, vol. 10, no. 1, pp. 16–28, Jan. 2019.
- [17] W. Liu, L. Sun, Z. Lin, F. Wen, and Y. Xue, "Multi-objective restoration optimisation of power systems with battery energy storage systems," *IET Gener., Transmiss. Distrib.*, vol. 10, no. 7, pp. 1749–1757, Apr. 2016.
- [18] L. Sun *et al.*, "Optimisation model for power system restoration with support from electric vehicles employing battery swapping," *IET Gener., Transmiss. Distrib.*, vol. 10, no. 3, pp. 771–779, Feb. 2016.
- [19] W. Liu, J. Zhan, C. Y. Chung, and L. Sun, "Availability assessment based case-sensitive power system restoration strategy," *IEEE Trans. Power Syst.*, vol. 35, no. 2, pp. 1432–1445, Mar. 2020.
- [20] Q. Zhang, Z. Ma, Y. Zhu, and Z. Wang, "A two-level simulation-assisted sequential distribution system restoration model with frequency dynamics constraints," *IEEE Trans. Smart Grid*, vol. 12, no. 5, pp. 3835–3846, Sep. 2021.
- [21] Y. Zhao, Z. Lin, Y. Ding, Y. Liu, L. Sun, and Y. Yan, "A model predictive control based generator start-up optimization strategy for restoration with microgrids as black-start resources," *IEEE Trans. Power Syst.*, vol. 33, no. 6, pp. 7189–7203, Nov. 2018.
- [22] X. Wu, S. Shi, X. Wang, C. Duan, T. Ding, and F. Li, "Optimal black start strategy for microgrids considering the uncertainty using a data-driven chance constrained approach," *IET Gener., Transmiss. Distrib.*, vol. 13, no. 11, pp. 2236–2248, Jun. 2019.
- [23] J. Zhao, Q. Wu, N. D. Hatziaargyriou, F. Li, and F. Teng, "Decentralized data-driven load restoration in coupled transmission and distribution system with wind power," *IEEE Trans. Power Syst.*, vol. 36, no. 5, pp. 4435–4444, Sep. 2021.
- [24] J. Zhao, H. Wang, Q. Wu, N. D. Hatziaargyriou, and F. Shen, "Optimal generator start-up sequence for bulk system restoration with active distribution networks," *IEEE Trans. Power Syst.*, vol. 36, no. 3, pp. 2046–2057, May 2021.
- [25] W. Liu and F. Ding, "Collaborative distribution system restoration planning and real-time dispatch considering behind-the-meter DERs," *IEEE Trans. Power Syst.*, vol. 36, no. 4, pp. 3629–3644, Jul. 2021.
- [26] C. Li, Y. Xu, J. He, P. Zhang, and L. Liu, "Parallel restoration method for AC-DC hybrid power systems based on graph theory," *IEEE Access*, vol. 7, pp. 66185–66196, 2019.
- [27] Z. Li, Y. Xue, H. Wang, and L. Hao, "Decision support system for adaptive restoration control of transmission system," *J. Modern Power Syst. Clean Energy*, vol. 9, no. 4, pp. 870–885, Jul. 2021.
- [28] M. Gutierrez, P. A. Lindahl, A. Banerjee, and S. B. Leeb, "An energy buffer for controllable input impedance of constant power loads," *IEEE Trans. Ind. Appl.*, vol. 55, no. 3, pp. 2910–2921, May/June 2019.
- [29] D. Rodriguez Medina *et al.*, "Fast assessment of frequency response of cold load pickup in power system restoration," *IEEE Trans. Power Syst.*, vol. 31, no. 4, pp. 3249–3256, Jul. 2016.
- [30] M. Song, R. R. Nejad, and W. Sun, "Robust distribution system load restoration with time-dependent cold load pickup," *IEEE Trans. Power Syst.*, vol. 36, no. 4, pp. 3204–3215, Jul. 2021.
- [31] C. Zhang, Z. Lin, F. Wen, Y. Xue, Q. Ni, and L. Ye, "A two-stage strategy for network reconfiguration based on concept of regret," *Automat. Electric Power Syst.*, vol. 37, no. 8, pp. 46–52, Apr. 2013.
- [32] R. Billinton and G. Singh, "Application of adverse and extreme adverse weather: Modelling in transmission and distribution system reliability evaluation," *IEE Proc.-Gener., Transmiss. Distrib.*, vol. 153, no. 1, pp. 115–120, Jan. 2006.
- [33] V. Chalishazar, S. Poudel, S. Hanif, and P. T. Mana, "Power system resilience metrics augmentation for critical load prioritization," Pacific Northwest Nat. Lab, Richland, WA, USA, Tech. Rep. PNNL-30837. [Online]. Available: <https://www.osti.gov/biblio/1764623-power-system-resilience-metrics-augmentation-critical-load-prioritization>
- [34] V. Chalishazar *et al.*, "Connecting risk and resilience for a power system using the Portland hills fault case study," *Processes*, vol. 8, no. 10, Sep. 2020, Art. no. 1200.
- [35] W. L. Winston, *Operations Research: Applications and Algorithms*, 4th ed. Toronto, ON, Canada: Thomson, 2003.
- [36] J. Lofberg, "YALMIP: A toolbox for modeling and optimization in MATLAB," in *Proc. IEEE Conf. Robot. Automat.*, Taipei, Taiwan, 2004, pp. 284–289.
- [37] Q. Zhang, Z. Wang, S. Ma, and A. Arif, "Stochastic pre-event preparation for enhancing resilience of distribution systems," *Renewable Sustain. Energy Rev.*, vol. 152, Dec. 2021, Art. no. 111636.
- [38] Y. Huang *et al.*, "Bi-level coordinated planning of active distribution network considering demand response resources and severely restricted scenarios," *J. Modern Power Syst. Clean Energy*, vol. 9, no. 5, pp. 1088–1100, Sep. 2021. doi: [10.1109/TPWRS.2020.3040130](https://doi.org/10.1109/TPWRS.2020.3040130).
- [39] V. Chalishazar *et al.*, "Data-driven reliability assessment for marine renewable energy enabled island power systems," in *Proc. IEEE Power Energy Soc. Gen. Meeting*, WA, DC, USA, 2021, pp. 1–5.
- [40] L. Ding, Y. Guo, P. Wall, K. Sun, and V. Terzija, "Identifying the timing of controlled islanding using a controlling UEP based method," *IEEE Trans. Power Syst.*, vol. 33, no. 6, pp. 5913–5922, Nov. 2018.
- [41] S. Maslennikov *et al.*, "A test cases library for methods locating the sources of sustained oscillations," in *Proc. IEEE Power Energy Soc. Gen. Meeting*, Boston, MA, USA, 2016, pp. 1–5.